

Appendix B

The 2013 Grand Passage Turbulence Experiment

Paper presented at the ICOE, Halifax, November 2014



VERTICAL PROFILES OF TURBULENCE METRICS IN GRAND PASSAGE, NOVA SCOTIA

Justine M. McMillan^{1*}, Alex E. Hay¹, Rolf G. Lueck² and Fabian Wolk²

¹Department of Oceanography, Dalhousie University, Halifax, Nova Scotia, Canada

²Rockland Scientific Inc., Victoria, British Columbia, Canada

*Email: justine.mcmillan@dal.ca

Abstract

The characterization of a tidal energy site requires the measurement of both the mean and turbulent aspects of the flow. In particular, an assessment of the turbulent characteristics can provide insight into the structural loading forces that would be applied to an installed turbine. The measurement of these dynamic, short-term variations in the flow is non-trivial. Most of the previous measurements in tidal channels have been made using acoustic instruments which have significant averaging, sampling rate and noise limitations. An alternative technology is the vertical microstructure profiler (VMP), which uses shear probes to obtain high-resolution vertical profiles of turbulent quantities, such as the rate of dissipation of turbulent kinetic energy (TKE). The dissipation rate provides critical information about the magnitude of the fluctuations associated with the turbulent flow.

This paper focuses on VMP measurements that were made in Grand Passage, Nova Scotia, which is located at the mouth of the Bay of Fundy. Using the VMP, 90 profiles of the vertical shear of horizontal velocity were measured at scales down to 3 mm. Transects were obtained in both the along- and cross-channel directions, which provided a quasi-synoptic view of the vertical and horizontal distribution of the dissipation rate, which ranged from 10^{-7} W/kg to 10^{-3} W/kg. This suggests a wide dynamic range of the turbulent kinetic energy, and hence, of the velocity fluctuations. The VMP also carried two fast-response thermistors, which provided measurements of the temperature microstructure and the vertical scale of overturns in the water column.

1 INTRODUCTION

Grand Passage, Nova Scotia, is located at the mouth of the Bay of Fundy. Tidal energy development in the channel is stimulated by a Community Feed-In Tariff (COMFIT) which permits the initial extraction of 0.5 MW of power. An assessment of the available resource has been ongoing since 2010 and has involved both flow measurements and numerical model simulations (Karsten and O'Flaherty-Sproul, 2013; McMillan et al., 2013; Hay et al., 2013). At several sites within the passage, the depth-averaged flow speed reaches 2 - 2.5 m/s and turbulence manifestations, such as boils and convergence zones, are often visible at the surface.

An understanding of the turbulence characteristics can provide insight into the structural loading forces that would be applied to a turbine. Information about the structure of the turbulence is therefore critical for the optimization of a turbine's design and the selection of its installation site. Previous, and ongoing, tidal energy site assessments have primarily used acoustic Doppler current profilers (ADCPs) and acoustic Doppler velocimeters (ADVs) to measure turbulence quantities (Thomson et al., 2012; Richard et al., 2013;

Milne et al., 2013; Hay et al., 2013). Despite their widespread use, these acoustic technologies have significant limitations, particularly related to their spatial resolution and high noise levels. The standard deviations associated with Doppler noise for both an ADCP and an ADV depend upon the sampling parameters, but typical manufacturer’s values for turbulence measurements are 0.156 m/s for an RDI 600 kHz Workhorse ADCP and 0.02 m/s for a Nortek Vector ADV (Thomson et al., 2012). Measured noise levels have been shown to agree well with the manufacturer’s values (Richard et al., 2013; Hay et al., 2013).

There are additional limitations of ADCPs and ADVs that are site specific. Firstly, both instruments require particulates to scatter the emitted acoustic signal. This was a major limitation in the use of an ADV in Grand Passage where correlations were low due to a lack of scatterers (Hay et al., 2013). Secondly, the use of an ADCP to measure turbulence in a region of complex bathymetry may violate the underlying assumption that the fluctuations in the flow are statistically homogeneous (Lu and Lueck, 1999). This is particularly problematic in deep channels (~ 50 m), where the beam spreading near the surface exceeds 30 m. The horizontal scales of bathymetric variability are typically less than the beam spread and, hence, the second order flow statistics in each of the beams can be significantly different, which violates the assumption of homogeneity. Errors in ADCP measurements of turbulent quantities can also be introduced due to instrument tilt angles as low as 2° (Lu and Lueck, 1999).

As an alternative, or perhaps a complement, to acoustic measurements of turbulence, shear probes can be used to measure the turbulent characteristics in the flow. These instruments have much lower noise levels (~ 0.001 m/s) and higher sampling rates (64 Hz) which make them capable of measuring velocity fluctuations at scales ranging from 0.003 – 1 m. This implies that for a typical dissipation rate of 10^{-4} W/kg (in a tidal channel), the turbulent velocity spectrum can be resolved to the transition from the inertial subrange to the dissipation range, which occurs at a length scale of approximately 10η , where η is the Kolmogorov microscale (~ 0.3 mm). Shear probes have been used to obtain vertical profiles of turbulence quantities in the open ocean for over 40 years, as summarized by Lueck et al. (2002); however, they have only recently been used for tidal energy applications (Lueck et al., 2013). In this paper, we will describe the measurement of turbulence metrics in Grand Passage using a Vertical Microstructure Profiler (VMP). In Section 2 we will describe the basic principles of the instrument and discuss its configuration for the Grand Passage measurements. We then summarize the calculation of the dissipation rate in Section 3 and discuss the results for Grand Passage in Section 4. Conclusions and final remarks are presented in Section 5.

2 THE AIRFOIL SHEAR PROBE AND THE VMP-200

The primary sensor on the VMP that measures turbulence is the airfoil shear probe, which is shown in Figure 1a. The probe, which is embedded into a hollow stainless steel support sting, consists of a piezo-ceramic element that is 13 mm long, 1.6 mm wide and 0.5 mm thick. There is a flexible, bullet-shaped, silicone rubber tip that encases the free end of the probe and forms an axially symmetric airfoil.

As the probe moves vertically through the water at speed, W , the horizontal component of the turbulent velocity, u , generates a lift force on the probe that causes the piezo-ceramic beam to bend microscopically. This induces a voltage, $e = SWu$, which depends on the sensitivity of the probe, S . The rate-of-change of u is calculated by

$$\frac{\partial u}{\partial t} = \frac{1}{SW} \frac{\partial e}{\partial t}. \quad (1)$$

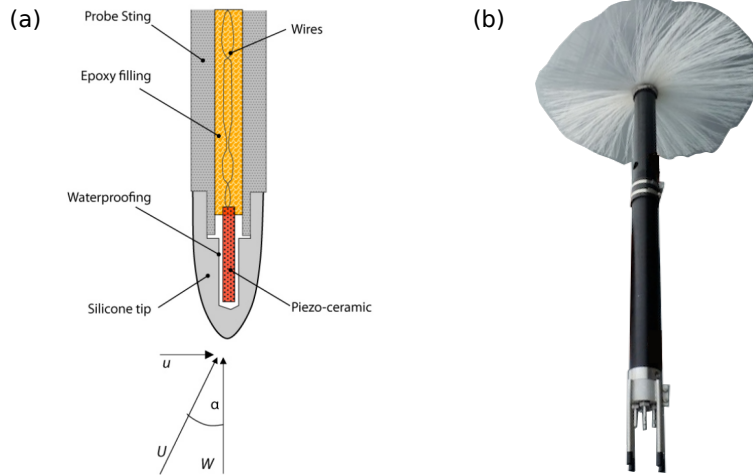


FIGURE 1: (a) Schematic of a shear probe. The apparent vertical velocity due to profiling, W , and the horizontal velocity fluctuation due to turbulence, u , result in a total velocity, U , and an angle of attack, α . (b) The VMP-200 shown here with a probe guard on the nose and a drag element on the tail.

The vertical shear is obtained by applying Taylor’s frozen field hypothesis, to yield

$$\frac{\partial u}{\partial z} = \frac{1}{SW^2} \frac{\partial e}{\partial t}. \quad (2)$$

Because the shear probe is only sensitive to the velocity fluctuations that are broadside to the piezo-beam, two probes are oriented at 90° to each other within the VMP. This allows for the measurement of both $\partial u/\partial z$ and $\partial v/\partial z$.

For this study, the *VMP-200* vertical profiler, which is shown in Figure 1b, was used. The profiler was developed by Rockland Scientific Inc. for use in coastal and shelf seas and is approximately 1.5 m long, 0.1 m in diameter and has a weight of 120 N in air. In addition to the shear probes, the VMP carried two high-resolution themistors, tilt sensors, accelerometers and a pressure transducer. Data was recorded internally on a memory card. The brushes on the tail of the instrument help to control both its fall rate and its righting moment. In comparison with its open-ocean operation, the VMP used in the tidal channel was heavier and had fewer brushes on its tail. Both these modifications increased the fall rate of the VMP, which therefore reduced the angle of attack, α , due to horizontal velocity fluctuations (see Figure 1a).

In total, 90 VMP measurements were made during both the flood and ebb tide on August 7th, 2013 at the locations shown in Figure 2. Throughout the study, a bottom mounted ADCP was situated in the centre of the passage. The ADCP was a 600 kHz RD Instruments Workhorse, sampling at 1.83 Hz (2-ping ensembles) in 0.5 m range bins. To avoid interference with other acoustic instruments on the same frame, the ADCP operated in burst mode, collecting approximately 7 minutes of data every 15 minutes. The depth-averaged flow speed as measured by the ADCP is shown in Figure 3a with the times corresponding to the VMP deployments shown in red. The mean horizontal velocity profiles during the VMP survey are shown in panels (b) and (c) of Figure 3. The asymmetry in the flow structure on the flood and ebb tide is due to the presence of a ridge about 500 m south of the ADCP position (see Figure 2).

The VMP was deployed from a drifting lobster fishing boat in a “tethered free-fall mode” where the profiler was connected to the ship by a line that had several metres of slack at the surface. This ensured that the tether did not affect the motion of the profiler, even as the ship and the profiler drifted apart. For a typical

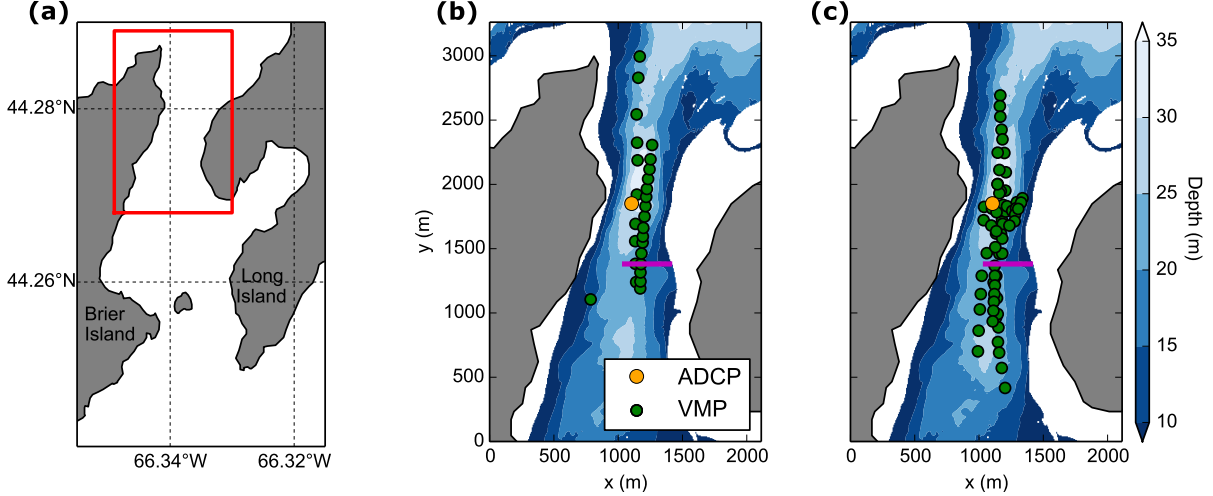


FIGURE 2: (a) Turbulence measurements were made at the northern end (red box) of Grand Passage, which is located between Brier Island and Long Island. The red rectangle corresponds to the enlarged region in (b) and (c). VMP deployment locations are plotted in (b) for the flood tide and (c) for the ebb tide. In both (b) and (c), the bathymetry is shown by the filled contours and the position of the ADCP is shown by the yellow marker. The magenta line identifies a ridge that generates significant asymmetry in the flow between the flood and ebb tides.

profile of ~ 20 m depth, the total horizontal drift of the VMP was estimated to be ~ 30 m due to falling rate of ~ 1.5 m/s and a mean flow speed of ~ 2 m/s. It should be noted that for fear of underestimating the depth, and consequently breaking the probes, each profile was terminated approximately 3-6 m above the bottom.

3 CALCULATION OF RATE OF DISSIPATION

The rate of dissipation, ϵ , of turbulent kinetic energy is the primary turbulence parameter that is computed from shear probe measurements. It describes the transfer of energy from the mean flow to the turbulent flow and its value is related to the magnitude of the turbulent velocity fluctuations. By definition, the dissipation rate is given by

$$\epsilon = \frac{1}{2} \nu \overline{\left(\frac{\partial u_i}{\partial x_j} + \frac{\partial u_j}{\partial x_i} \right) \left(\frac{\partial u_j}{\partial x_i} + \frac{\partial u_i}{\partial x_j} \right)}, \quad (3)$$

where ν is the kinematic viscosity and repeated indices represent summation notation. The overline represents a temporal average over a timescale such that the mean of the velocity fluctuations is zero. Because a tidal channel is typically well-mixed, it can be assumed that stratification is unimportant and hence the turbulent velocity fluctuations are nearly isotropic. This reduces equation (3) to

$$\epsilon = \frac{15}{2} \nu \overline{\left(\frac{\partial u}{\partial z} \right)^2} = \frac{15}{2} \nu \int_0^\infty \psi(k) dk, \quad (4)$$

where k is the wavenumber and $\psi(k)$ is the spectrum of the shear. The second equality arises because the variance of a signal is equal to the integral of its spectrum.

The shear measurements from two profiles are shown in Figure 4, where both a weakly-turbulent and a

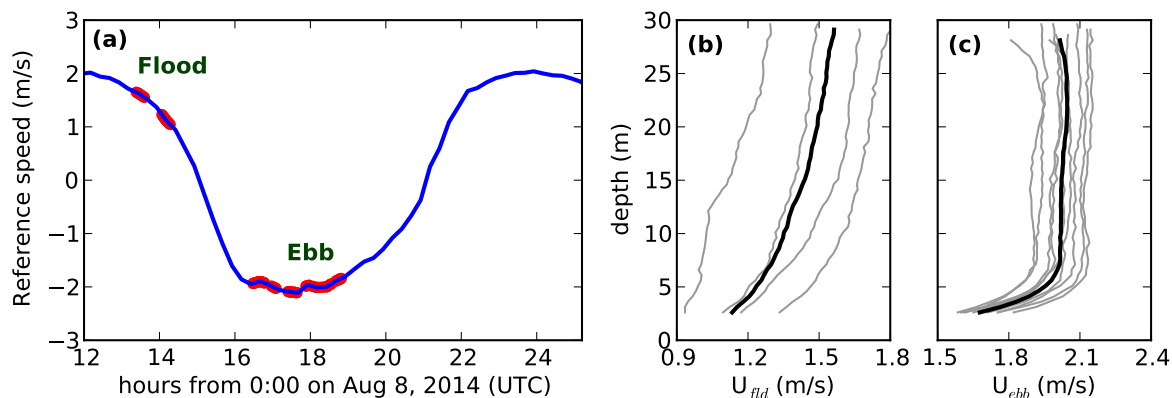


FIGURE 3: (a) The times at which VMP profiles were made with reference to the depth-averaged horizontal flow speed as measured by the nearby ADCP. (b) The velocity profiles as measured by the ADCP during the times of the VMP deployments on the flood tide. The grey lines are the 15 minute ensembles and the black line indicates the mean. (c) Same as (b), except for the ebb tide.

strongly-turbulent region are highlighted. The raw data are shown in the left most panel, and the dissipation rate estimates are shown in the middle panel. To obtain the ϵ values for the Grand Passage data, each profile was analysed in 2 s segments, which overlapped by 1 s. This resulted in a vertical resolution of approximately 1.5 m for ϵ (See Section 4.1). For each 2 s segment, the frequency spectrum was computed using 0.5 s intervals with 50% overlap. The frequency spectra were then converted to wavenumber spectra using Taylor’s frozen field hypothesis and corrections were made for both the spatial averaging introduced due to the physical size of the shear probe (Macoun and Lueck, 2004) and for the vibration of the profiler (Goodman et al., 2006). Two examples of the resulting spectra are shown in the right-most panel of Figure 4. For the smaller wavenumbers ($k < 12$ cpm), both spectra exhibit a well-defined inertial subrange where $\psi \sim k^{1/3}$, as predicted by Kolmogorov.

One of two methods is employed to compute the dissipation rate from the shear spectra. For low signal-to-noise ratios (i.e. low turbulence intensities), the upper limits of integration, k_{max} , (shown by the triangles) are chosen so that the noise dominated region ($k > k_{max}$) of the spectra is excluded. Since the spectral values at the cutoff wavenumber, $\psi(k_{max})$, are about 10 times lower than ψ_{max} , truncating the upper limit of integration does not significantly affect the estimate of ϵ . For higher signal-to-noise ratios (i.e. high turbulence intensities), as in the lower panel, the spectral values do not decrease significantly before the attenuation effects of the anti-aliasing filters dominate the spectrum ($k \approx 150$ cpm). Integration of the spectra would therefore result in an under estimation of the ϵ values. For these measurements, ϵ was estimated from the best fit to the Nasmyth empirical spectrum (Nasmyth, 1970; Oakey, 1982; Wolk et al., 2002) in the $k < k_{max}$ region. As shown by the black lines in Figure 4, the Nasmyth spectra agree well with the measurements for $k < 10^2$ cpm. In the weakly turbulent region (top panel), the Nasmyth spectrum extends into the dissipation range.

4 RESULTS

In this section, we present the results for the VMP deployments made in Grand Passage (Figure 2). We will first discuss the kinematic behaviour of the instrument in the energetic channel and then analyse the

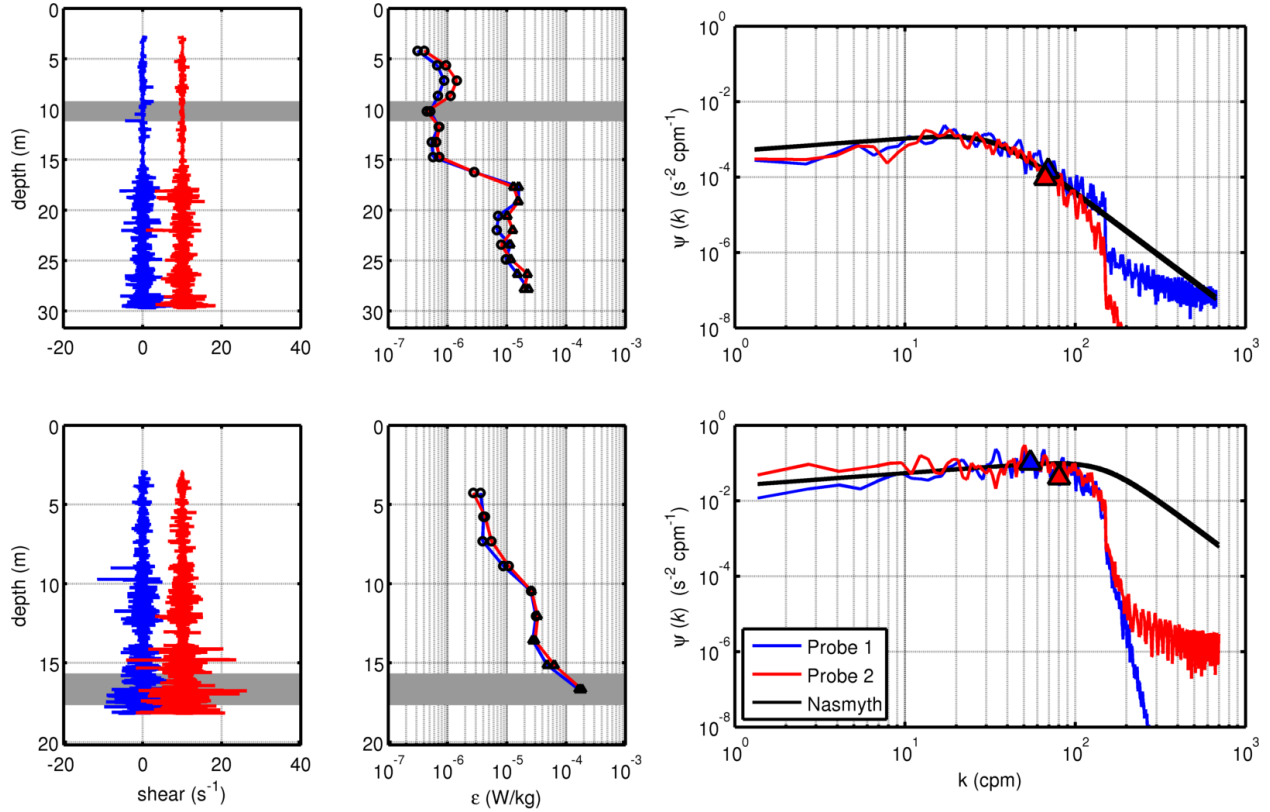


FIGURE 4: Computation of shear spectra from a weakly-turbulent region (top row) and a strongly-turbulent region (bottom row). In all the plots, the blue and red lines correspond to probes 1 and 2, respectively. The left-most panel shows the raw shear measurements with the measurements from probe 2 offset by 10 s^{-1} for clarity. The middle panel shows the computed dissipation rate with the markers indicating the method that was used. Circles correspond to the integration of the spectrum up to the integration limit and triangles correspond to the fitting of the Nasmyth curve within its $k^{1/3}$ region. The right-most panel shows the spectra corresponding to the grey regions in the other plots. The triangles indicate the maximum wavenumbers that were used in the determination of ϵ for the integration method (top panel) and the Nasmyth fitting method (bottom panel). The black lines represent the Nasmyth curves for the computed dissipation rate.

turbulence measurements with a focus on the spatial variability of the dissipation rate within the channel.

4.1 KINEMATIC BEHAVIOUR OF THE VMP

The behaviour of the VMP was assessed by analyzing both the fall rate, W , and the inclination angle, θ , of the instrument. The fall rate was computed from the rate-of-change of pressure and the inclination angle was measured with respect to the vertical. An example of the variation of W and θ with depth, d , is shown in Figure 6a. For all profiles, the VMP typically fell at a semi-constant speed between $5 \text{ m} < d < d_{max} - 3 \text{ m}$, where d_{max} is the depth at which the profile was terminated. Statistical quantities were therefore computed within this range of depths.

The average falling rate amongst all profiles was 1.5 m/s and the distribution is plotted in Figure 5a. Within a given profile, the standard deviation of the vertical velocity was always less than 9 cm/s (Figure 5b). The largest variations in W occurred in regions of high shear where the presence of up-drafts and down-drafts likely affected the motion of the profiler. Because the profiler reaches its terminal velocity within one

body length, it adjusts quickly to any up- or down-draft; therefore, the speed of the flow past the VMP is always close to the typical fall rate, W .

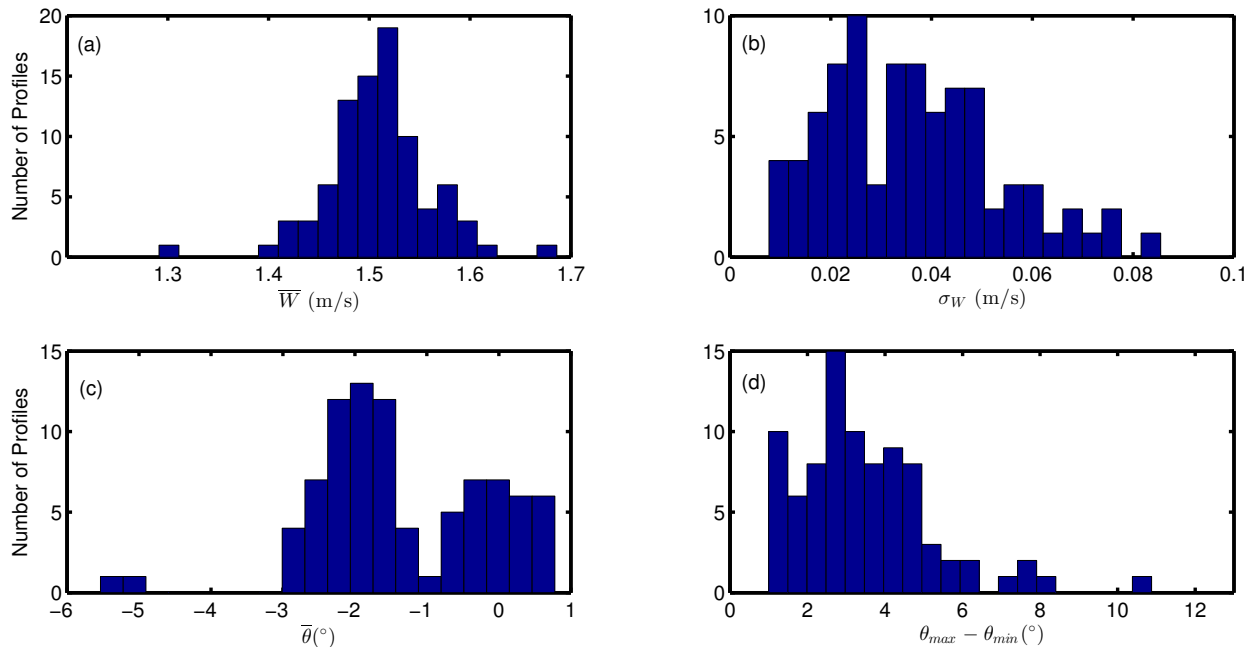


FIGURE 5: Histograms summarizing the kinematic behaviour of the VMP where all quantities were determined between depths of 5 m and $d_{max} - 3$ m. (a) The mean fall rate, \bar{W} . (b) The standard deviation, σ_W , of the fall rate. (c) The mean inclination angle, $\bar{\theta}$. (d) The range, $\theta_{max} - \theta_{min}$, of inclination angle.

The average inclination angle amongst all profiles was -1.35° . The distribution of the means is shown in Figure 5c. The range in θ (i.e. $\theta_{max} - \theta_{min}$) is plotted in Figure 5d. The average range was 3.4° , with most of the profiles having a range less than 5° . Proper operation of the shear probe requires that the angle of attack, α , due to fluctuations of horizontal velocity remains within $\pm 20^\circ$ (Osborn and Crawford, 1980). Large pitching motions could violate this assumption.

4.2 THERMISTOR MEASUREMENTS

The VMP had two thermistors which measured temperature to a resolution of 0.02 m. As shown by the example profile in Figure 6b, the water column is fairly well mixed with the overall range of only about 0.2°C in temperature. At this particular location, the water is slightly warmer in the upper 10 m compared to the lower 10 m. Furthermore, the temperature gradients, which are shown in Figure 6c, indicate that the lower portion of the water column is fully mixed. The variability in T_1 and T_2 between 11 m and 13 m suggests a possible overturning event which corresponds to the depth at which the velocity shear, and hence dissipation rate, begins to increase. The temperature measurements are a useful tracer for water masses and can be used to estimate the vertical scale of overturning.

4.3 SPATIAL VARIATION OF DISSIPATION RATE

For this study, vertical profiles were obtained at numerous locations throughout the northern end of the passage during one flood tide and one ebb tide (Figure 2). Despite the sampling region being only about

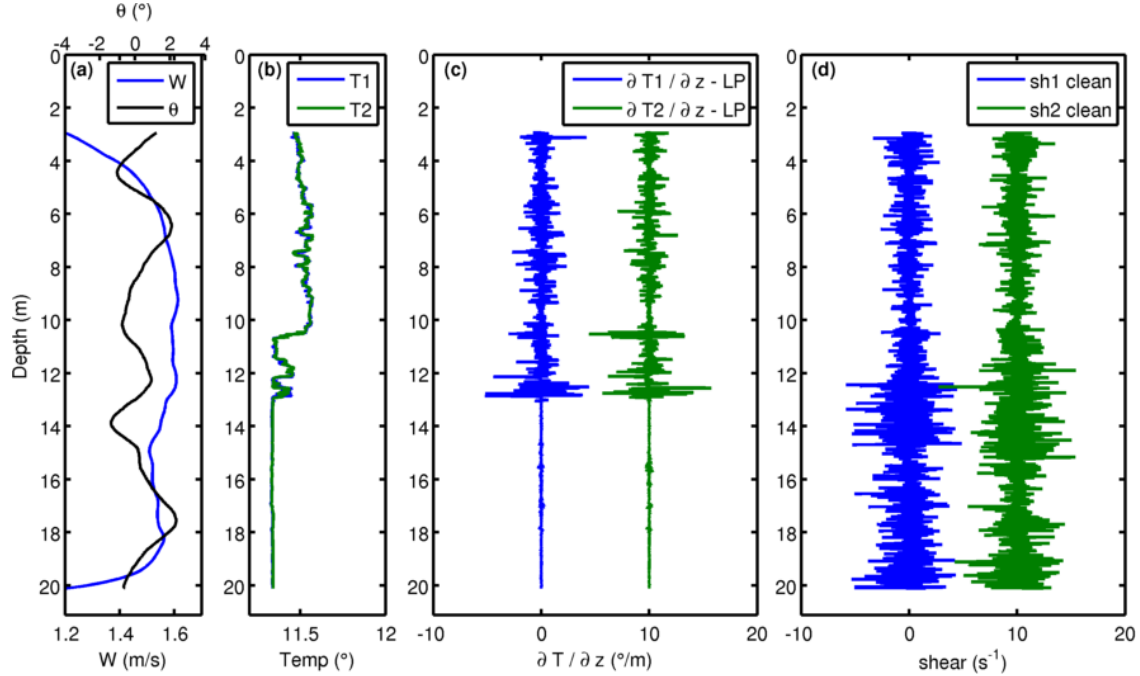


FIGURE 6: Data collected during one vertical profile. (a) The falling rate, W , and the inclination angle, θ , of the VMP with respect to the vertical. (b) Temperature as measured by the two thermistors. (c) Low pass filtered temperature gradients. (d) Despiked vertical shear measurements.

2 km² in size, there was significant variation in the dissipation rates as shown by the transects in Figure 7. On the flood tide (Figure 7a), the dissipation rate is the highest immediately upstream of a ridge which is located at ~ 150 m. Downstream of the ridge, the dissipation rates are approximately an order of magnitude higher near the bed than near the surface. On the ebb tide (Figure 7b), the dissipation rate is low at the northern end of the passage. As the flow approaches the ridge, the turbulence levels increase throughout the water column and remain high downstream of the ridge. Overall, the dissipation rate is higher on the ebb tide compared with the flood; however, the VMP measurements were made during stronger flows on the ebb tide. The cross-channel transect, which is shown in Figure 7c shows that the dissipation rate varies significantly over the 200 m region with the largest ϵ values being measured on the eastern side of the passage where the bathymetric gradient is larger.

4.4 COMPARISON TO OTHER INSTRUMENTS

Using the method of Hay et al. (2013), the average ϵ value as measured by the nearby ADCP was computed as a function of the mean flow speed at 10 m above the bottom. For speeds ranging from 1.8 - 2 m/s, ϵ was approximately 4×10^{-5} W/kg on the flood tide and 5×10^{-6} W/kg on the ebb tide. More work needs to be done to make direct comparisons between the ADCP and VMP results, however, it does appear that the two instruments obtain the same order of magnitude for the dissipation rate.

5 CONCLUSIONS

The characterization of turbulence at a tidal energy site is crucial for understanding the forces that will be exerted on an underwater turbine. Most site assessments rely on the use of acoustic instruments (e.g.

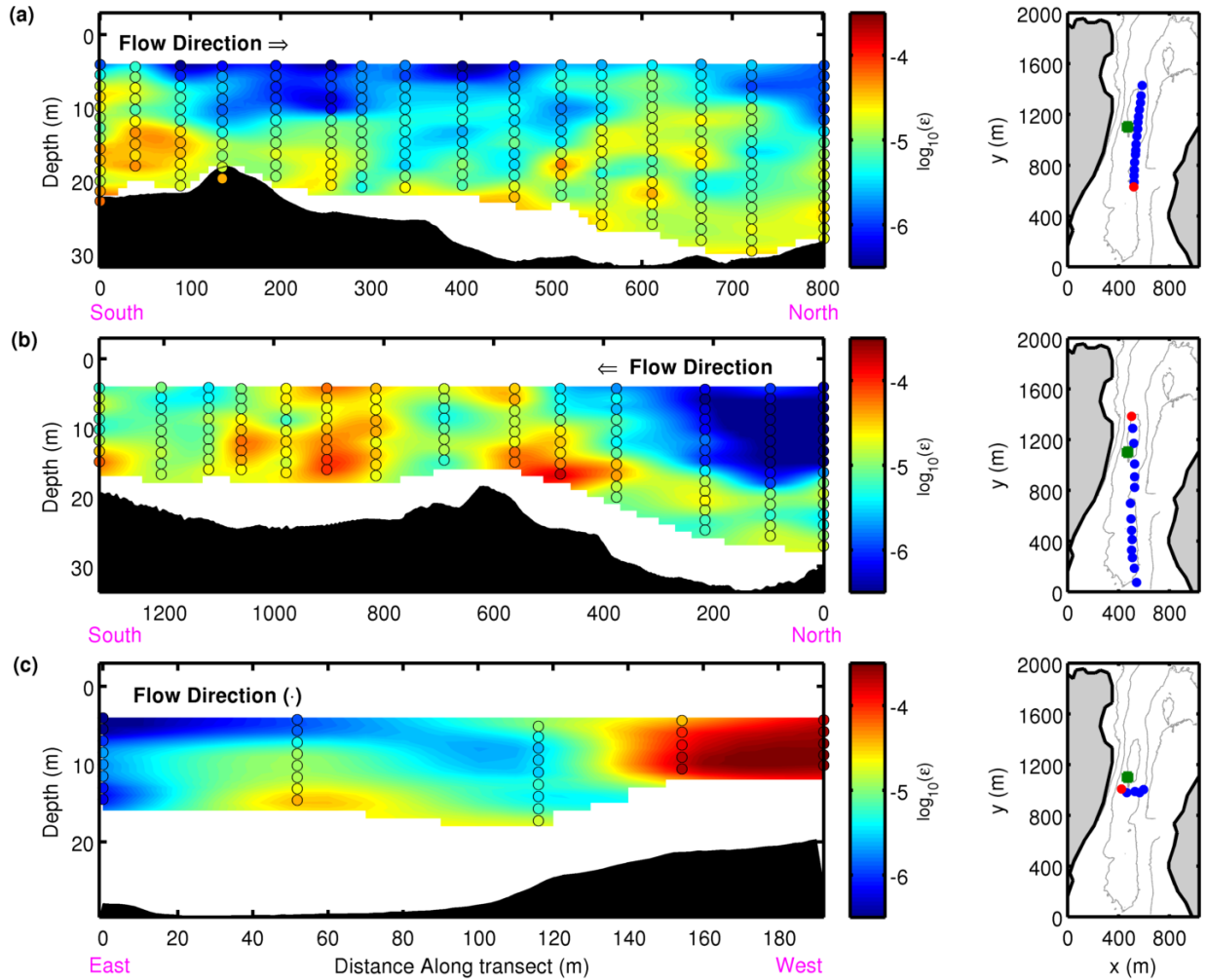


FIGURE 7: The dissipation rate measured on along-channel transect during the (a) flood and (b) ebb tides, and (c) during a cross channel transect on the ebb tide. For each transect, the coloured points in the left panel correspond to the profiles from which the transect was interpolated. The bathymetry along the transect is shown by the black region. The right panels show the geographical locations of the profiles (blue points) with the reference location shown in red. The ADCP location is shown by the green square.

ADCPs and ADVs) for the measurement of both the mean flow and the turbulent fluctuations; however, these instruments have several limitations that could lead to an inaccurate assessment of the turbulence levels. In this paper, we have shown that the use of a vertical microstructure profiler can provide high resolution measurements of the horizontal shear. Used together, shear probe and acoustic measurements could be used to assess the flow at all the relevant scales.

The VMP measurements have allowed for an analysis of the spatial variation in the dissipation rate throughout Grand Passage. The ϵ values ranged from 10^{-7} to 10^{-3} W/kg with the largest values found on the eastern side of the passage. Vertical profiles of the dissipation rate indicated that the turbulence levels were typically the highest near the seabed and in the vicinity of a bathymetric ridge.

As the research progresses, the temporal variation of ϵ will be examined using shear probes mounted on a streamlined buoy “flown” at mid-depth. This will allow for an assessment of the variation of ϵ over several

tidal cycles at a nominal “hub height”. It will also allow for further comparison with ADCP measurements.

6 ACKNOWLEDGEMENTS

We thank Richard Cheel, Greg Trowse, and Peter Stern for assistance in the field. We also acknowledge Reid Gillis who captained the *Island Lady G* during the completion of this work. Funding was provided by the Offshore Energy Research Association and the Natural Sciences and Engineering Research Council.

References

- Goodman, L., Levine, E. R., and Lueck, R. G. (2006). On measuring the terms of the turbulent kinetic energy budget from an AUV. *Journal of Atmospheric and Oceanic Technology*, pages 977–990.
- Hay, A. E., McMillan, J. M., Cheel, R., and Schillinger, D. J. (2013). Turbulence and drag in a high Reynolds number tidal passage targetted for in-stream tidal power. In *Oceans 2013 San Diego*, pages 1–10.
- Karsten, R. and O’Flaherty-Sproul, M. (2013). Numerical modelling of Digby Neck tidal currents. Technical report, OERA.
- Lu, Y. and Lueck, R. G. (1999). Using a broadband ADCP in a tidal channel. Part II: Turbulence. *Journal of Atmospheric and Oceanic Technology*, pages 1568–1579.
- Lueck, R. G., Wolk, F., and Black, K. (2013). Measuring tidal channel turbulence with a vertical microstructure profiler (VMP). Technical Report 1, Rockland Scientific Inc.
- Lueck, R. G., Wolk, F., and Yamazaki, H. (2002). Oceanic velocity microstructure measurements in the 20th century. *Journal of Oceanography*, 58:153–174.
- Macoun, P. and Lueck, R. G. (2004). Modeling the spatial response of the airfoil shear probe using different sized probes. *Journal of Atmospheric and Oceanic Technology*, pages 284–297.
- McMillan, J. M., Hay, A. E., Karsten, R. H., Trowse, G., Schillinger, D. J., and O’Flaherty-Sproul, M. (2013). Comprehensive tidal energy resource assessment in the lower Bay of Fundy, Canada. In *10th European Wave and Tidal Energy Conference*, pages 1–10.
- Milne, I. A., Sharma, R. N., Flay, R. G. J., and Bickerton, S. (2013). Characteristics of the turbulence in the flow at a tidal stream power site. *Phil Trans R Soc A*, 371(January):1–14.
- Nasmyth, P. W. (1970). *Oceanic Turbulence*. Phd, University of British Columbia.
- Oakey, N. S. (1982). Determination of the rate of dissipation of turbulent energy from simultaneous temperature and velocity shear microstructure measurements. *Journal of Physical Oceanography*, 12:256–271.
- Osborn, T. R. and Crawford, W. R. (1980). An airfoil probe for measuring turbulent velocity fluctuations in water. In Dobson, F., Hasse, L., and Davis, R., editors, *Air-Sea Interaction*, pages 369–386. Plenum Press.
- Richard, J. B., Thomson, J., Polagye, B., and Bard, J. (2013). Method for identification of Doppler noise levels in turbulent flow measurements dedicated to tidal energy. *International Journal of Marine Energy*, 3-4:52–64.
- Thomson, J., Polagye, B., Durgesh, V., and Richmond, M. C. (2012). Measurements of turbulence at two tidal energy sites in Puget Sound, WA. *IEEE Journal of Oceanic Engineering*, 37(3):363–374.
- Wolk, F., Yamazaki, H., Seuront, L., and Lueck, R. G. (2002). A new free-fall profiler for measuring bio-physical microstructure. *Journal of Atmospheric and Oceanic Technology*, 19:780–793.